MONTE-CARLO ANALYSIS OF THE PULSED ELECTROSTATIC TRACTOR STRENGTH

Joseph Hughes and Hanspeter Schaub

14th Spacecraft Charging Technology Conference

ESA/ESTEC, Nederland **April 4–8, 2016**

MONTE-CARLO ANALYSIS OF THE PULSED ELECTROSTATIC TRACTOR STRENGTH

Joseph Hughes[1] **and Hanspeter Schaub**[2]

[1] *University of Colorado, Aerospace Engineering Sciences Department, ECEE 275, 431 UCB, University of Colorado, Boulder, CO, USA, 80309-0431, Joseph.Hughes@Colorado.edu*

[2] *University of Colorado, Aerospace Engineering Sciences Department, ECNT 321, 431 UCB, University of Colorado, Boulder, CO, USA, 80309-0431, Hanspeter.Schaub@Colorado.edu*

ABSTRACT

If a constant-current electron beam mounted on a tug spacecraft irradiates a passive debris object, the tug quickly rises to a positive steady-state voltage and the debris quickly falls to a negative steady-state voltage. A Coulomb force draws the two objects together and has been considered as a means of touchless actuation for Geosyncronous debris re-orbiting, de-tumbling, and formation flying. This paper expands this concept to use a beam with time-varying current. A Monte Carlo analysis of the force, accelerations, re-orbiting time, power requirements, and feasibility of a pulsed Electrostatic Tractor (ET) are presented. Voltage and power regimes are identified where the pulsed ET implementation provides a stronger force then a continuous beam ET.

Key words: Electrostatic Tractor; Orbital Debris; Re-Orbiting.

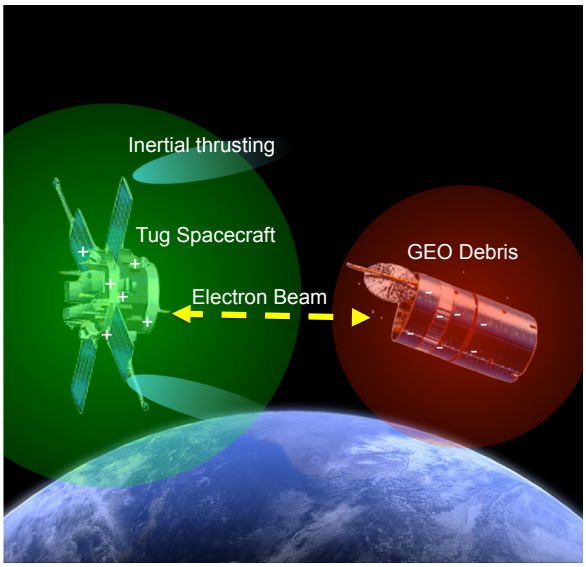

Figure 1. The Electrostatic Tractor (ET) allows spacecraft to touchlessly exert forces and torques on passive space objects

1. INTRODUCTION

The Geosynchronous (GEO) orbit regime is home to at least $18.3 Billion in space assets from the civil, commercial, and defense sectors [5] Of the 1369 tracked objects in GEO, only 21% are controlled. This crowding of large, often school-bus sized objects creates the probability of collision, which is expected to worsen with current launch and de-orbiting trends. To reduce the collision probability, many concepts have been proposed to move GEO debris into a graveyard orbit about 200 – 250 km above GEO.

One such concept is the Electrostatic Tractor (ET) [12, 8, 16], which uses an electron beam to charge a tug spacecraft positive and a debris object negative. An attractive Coulomb force results from this charging. For two moderately sized spacecraft (3m diameter) charged at $\pm$20 kV, and separated by 7 craft radii, the debris feels a 1.2 mN force that could raise its orbit by more than 5 km/day [17]. A tug craft equipped with an electron gun and low thrust motors could move defunct GEO satellites to a graveyard orbit in a matter of months [17] where they would no longer pose a collision threat in a very valuable but threatened orbital region[1, 2]. Additionally, spacecraft with non-symmetric charge distributions will also feel and apply torques through this charging [4, 19, 20]. This torque can be used to touchlessly detumble non-cooperative space objects in a matter of days [3].

Charging to the needed levels is feasible, as spacecraft naturally charge to 10's of kilovolts in shaded GEO conditions [6]. Interactions between this charge and the Earth's magnetic field can cause significant perturbations especially for High-Area-to-Mass-Ratio (HAMR) objects [7]. These perturbations can be harnessed for orbit changes [13, 14, 22] without using chemical propellant.

This paper augments the ET concept by using a pulsed

electron beam rather than a continuous one. This change greatly expands the complexity of the analysis, but yields increased force at the same power level in many cases and allows for windows in which the beam is not operating and both craft are discharged to use control thrusters and make observations.

2. PROBLEM STATEMENT

2.1. Charging Model

A spacecraft is subject to many environmental currents as well as a pulsed electron beam. The environmental currents are a function of the space plasma parameters and the voltage of the spacecraft (ϕ), and the electron beam is a function of time. The temporal rate of change of charge is the sum of the currents, which yields a forced ordinary differential equation for the charge on a spacecraft.

$$\frac{\mathrm{d}q}{\mathrm{d}t} = I_{\text{beam}}(t) + \sum I_{\text{env}}(\phi) \tag{1}$$

$$= I_{\text{e}}(\phi, A) + I_{\text{i}}(\phi, A) + I_{\text{p}}(V, A) + I_{\text{SEE}}(\phi_{\text{eff}}) + I_{\text{beam}}(\phi, t) \tag{2}$$

Where the environmental currents (I_{env}) are the electron plasma current I_e, plasma ion current I_i, photoelectric current I_p, beam current I_b and secondary electron emission current I_{SEE}. Backscattering also plays a role in this charging, and further work will investigate it's effect. Each of the currents are next described individually.

2.1.1. Electron Plasma Current

In a typical GEO plasma, the thermal energy of the electrons corresponds to speeds close to 10^7 m/s. Some of these electrons impact the spacecraft and cause a negative current to the spacecraft. A model for the electron plasma current is given by [11]:

$$I_{\text{e}} = \begin{cases} -\dfrac{Aqn_e v_{\text{th}_{\text{e}}}}{4} e^{q\phi/k_{\text{B}}T_{\text{e}}} & \phi < 0 \quad (3) \\ -\dfrac{Aqn_{\text{e}} v_{\text{th}_{\text{e}}}}{4}(1 - \dfrac{q\phi}{k_{\text{B}}T_{\text{e}}}) & \phi \geq 0 \quad (4) \end{cases}$$

Where I_{e} is the electron plasma current [A], A is the spacecraft area [m^2], q is the fundamental charge [C], n_{e} is the electron density [#/m^3], $v_{\text{th}_{\text{e}}}$ is the root mean square electron thermal speed [m/s], which is given for either species by $v_{\text{th}} = \sqrt{8k_{\text{B}}T/\pi m}$. The spacecraft energy is $q\phi$ [eV], and $k_{\text{B}}T_{\text{e}}$ is the electron thermal energy [eV].

2.1.2. Ion Plasma Current

The ion plasma current is a result of the ions impacting the spacecraft, absorbing an electron, and leaving the system. The model is similar to the electron plasma current with a polarity flip [11].

$$I_i = \begin{cases} -\dfrac{Aqn_{\text{i}} v_{\text{th}_{\text{i}}}}{4} e^{q\phi/k_{\text{B}}T_{\text{i}}} & \phi > 0 \quad (5) \\ -\dfrac{Aqn_{\text{i}} v_{\text{th}_{\text{i}}}}{4}(1 - \dfrac{q\phi}{k_{\text{B}}T_{\text{i}}}) & \phi \leq 0 \quad (6) \end{cases}$$

Where $v_{\text{th}_{\text{i}}}$ and $k_{\text{B}}T_{\text{i}}$ are the ion thermal speed [m/s] and thermal energy [eV], respectively. For both ions and electrons, the current absorbed from the attracted species is linear in voltage, and the current from the repulsed species exponentially decays with voltage.

2.1.3. Photoelectron Current

Energy from the sun can energize electrons in the first few nanometers of the spacecraft surface so that they leave the surface of the craft. The fraction that have enough energy to escape the potential well of the spacecraft cause a net positive current given by [11]:

$$I_p = \begin{cases} j_{\text{ph}} A_\perp e^{-q\phi/k_{\text{B}}T_{\text{ph}}} & \phi > 0 \quad (7) \\ j_{\text{ph}} A_\perp & \phi \leq 0 \quad (8) \end{cases}$$

Where j_{ph} is the photoelectron flux [A/m^2], $A_\perp$ is the illuminated area [m^2], and $k_{\text{B}}T_{ph}$ is the thermal energy of the ejected photoelectrons [eV]. For a negative spacecraft this current is constant, and for a positively charged spacecraft it vanishes quickly.

2.1.4. Electron Beam

If a beam of electrons is shot from the tug craft to the deputy craft, it will cause a positive current on the tug and a negative current on the deputy. If the beam does not have sufficient energy to escape the potential well of the tug, it will return and cause no net currents. If it has sufficient energy to leave the well of the tug, but insufficient energy to reach the deputy, it will stop short and reverse it's direction. These electrons have sufficient energy to escape the system, but some may impact the tug before they have a chance to escape. Further analysis is needed to quantify the fraction that do not escape, but in this analysis we assume that it is negligible. The currents on the deputy are then given by:

$$I_{\text{bd}} = \begin{cases} -I_{\text{b}} & V_{\text{b}} > \phi_{\text{T}} - \phi_{\text{D}} \quad (9) \\ 0 & V_{\text{b}} < \phi_{\text{T}} - \phi_{\text{D}} \quad (10) \end{cases}$$

Where I_{bd} is the beam current on the deputy [A], V_b is the accelerating voltage of the beam [V], and ϕ_t and ϕ_d are the potentials of the tug and deputy spacecraft, respectively. The currents on the tug are given by:

$$I_{\text{bt}} = \begin{cases} I_{\text{b}} & V_{\text{b}} > \phi_{\text{T}} \quad (11) \\ 0 & V_{\text{b}} < \phi_{\text{T}} - \phi_{\text{D}} \quad (12) \end{cases}$$

2.1.5. Secondary Electron Emission

When an energetic particle impacts a material, it can eject neighboring electrons to cause a positive current. This current is only a consideration for the deputy craft. The secondary electron emission (SEE) current is modeled as:

$$I_{\text{SEE}} = \begin{cases} -4Y_{\text{M}} I_{\text{bd}}\,\kappa & \phi_{\text{D}} < 0 \quad (13) \\ 0 & \phi_{\text{D}} \geq 0 \quad (14) \end{cases}$$

Where Y_{M} is a material property that describes the maximum yield of secondary electrons, κ is scaling factor based on the effective energy of the beam $V_{\text{eff}} = V_{\text{b}} - \phi_{\text{T}} + \phi_{\text{D}}$, and V_{max} is a material property.

$$\kappa = \frac{V_{\text{eff}}/V_{\text{max}}}{(1 + V_{\text{eff}}/V_{\text{max}})^2} \quad (15)$$

This is a positive current with a maximum equal to Y_{M} multiplied by the incident current that occurs when $V_{\text{eff}} = V_{\text{max}}$. Y_{M} is larger than 1 for many materials, which means that an electron beam can actually charge a spacecraft positively.

2.2. Position Dependent Capacitance

All of the currents in the earlier subsection are functions of voltage, not charge. Since the fundamental state is charge, we must translate this charge to voltage to calculate the currents and update the state. The voltage of each spacecraft is a function of its own charge and the charge of nearby spacecraft. If we assume two spherical spacecraft separated by ρ which is constrained to be larger than both spacecraft radii $R_{\text{D}}, R_{\text{T}}$ the relation becomes:

$$\begin{bmatrix} \phi_{\text{T}} \\ \phi_{\text{D}} \end{bmatrix} = \frac{1}{4\pi\epsilon_0} \begin{bmatrix} 1/R_{\text{T}} & 1/\rho \\ 1/\rho & 1/R_{\text{D}} \end{bmatrix} \begin{bmatrix} q_{\text{T}} \\ q_{\text{D}} \end{bmatrix} \quad (16)$$

Where ϕ_{T} and ϕ_{D} are the absolute potentials of the tug and debris, respectively. This is used at each time step to calculate the voltages which are used to calculate the currents.

2.3. Force Model

The force between two point charges separated by ρ is given by [9]:

$$\boldsymbol{F} = \frac{q_{\text{D}}\, q_{\text{T}}}{4\pi\epsilon_0 \rho^2} \hat{\boldsymbol{\rho}} \quad (17)$$

In this analysis we neglect Debye shielding because the Debye length at GEO (200 m) is larger than our spacecraft separation (15 – 50 m). Because craft voltages are often much higher than the electron temperature, a key assumption in the standard Debye shielding development is violated. Stiles et. al. [21] found effective Debye lengths to be much larger which lends support to neglecting shielding for this analysis.

For the pulsed ET, the pulsing frequency is on the order of Hz, which is much faster than the orbital frequency of μHz. This allows us to use the average force as continuous for the purposes of orbit raising.

3. METHODS

In this analysis, nominal GEO space weather conditions and approximate material property values were used. This is shown in Tab. 1:

Table 1. Nominal GEO space weather parameters and approximate material property values

Parameter	Value
j_{ph}	20 μA/m^2
$k_{\text{B}}T_{\text{ph}}$	2 eV
n_{e}	0.6 cm^{-3}
n_{i}	9.5 cm^{-3}
$k_{\text{B}}T_{\text{e}}$	1250 eV
$k_{\text{B}}T_{\text{i}}$	50 eV
V_{max}	300 V
Y_{M}	2

3.1. Pulsed Beaming Fundamentals

A program is written to find the currents as a function of both the spacecraft charge levels and time. This is used to propagate the state $[q_1, q_2]^T$ through time using an RK4 integrator. This is shown explicitly below:

$$\begin{bmatrix} \dot{q}_{\text{T}} \\ \dot{q}_{\text{D}} \end{bmatrix} = \begin{bmatrix} \sum I_{\text{T}}(q_{\text{T}}, q_{\text{D}}, t) \\ \sum I_{\text{D}}(q_{\text{T}}, q_{\text{D}}, t) \end{bmatrix} \quad (18)$$

Auxiliary variables of $\boldsymbol{\phi}(t) = [\phi_T(t), \phi_D(t)]^T$ and $F(t)$ are also recorded.

3.2. Pulsed Beaming Monte Carlo Optimization

This paper examines the effect of varying the pulsed beam parameters to optimize the force and semi-major axis (SMA) rate. For this paper we consider a square wave which has four parameters: voltage (V_b), Current (I_b), Period (T_p) and Duty Cycle (d). Varying the tug (R_{T}) and debris (R_{D}) sizes increases the search space to six independent parameters. These parameters are randomized within the bounds shown below and fed into the integrator described above. The average force in the case of the pulsed beams and the final force for the continuous cases is computed for each run and stored in a master file along with the parameters that produced it.

Parameter	Lower Limit	Upper Limit
R_T	1.5 m	5m
R_D	1.5 m	5m
V_b	5 kV	100 kV
I_b	50 μA	10 mA
T_p	100 ms	1 s
d	0.01	0.99

A center-to-center distance r of $5(R_T + R_D)$ is used. This gives 4 craft diameters of standoff distance (12 m to 40 m). Since many GEO spacecraft have large solar panels and may be rotating, even this distance will require very careful formation flying. The integration time was constrained to be the larger of 10 pulse periods or 0.1 seconds. The time step is chosen so that either there are 50 steps in the "on" segment of the perid, or that the beam cannot change either craft voltage by more than a kV during one step. This results in a time step that can vary from 16 μs to 20 ms. Ten thousand runs were computed, five thousand for the pulsed ET and five thousand for the continuous ET.

4. FORCE ANALYSIS

The average force produced by a pulsed beam is plotted against the final force of a continuous beam in Fig. 2. Points below the hypothetical line with slope equal to 1 represent parameter sets (R_T, R_D, V_b, I_b, T_p, and d) where the average force was higher for the continuous beam (setting d equal to 1).

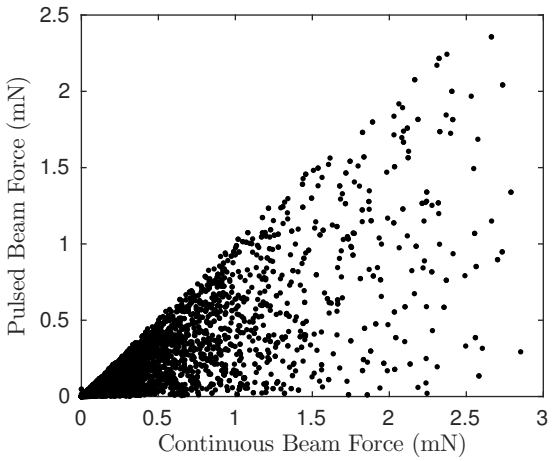

Figure 2. Comparison of forces produced by continuous and pulsed beams with all other parameters equal

As expected, there are far more points below the line than above it, as the force decays once the beam is turned off. As for the magnitude of the forces, we see definite improvements over prior work. There are multiple parameter sets that produced forces larger than 2 mN, in contrast Hogan et. al [10] found forces less than 1 mN, but used a more conservative beam voltage.

If we consider a power-limited tug, the pulsed ET begins to show its worth. The power in the beam can be expressed as $P = V_b I_b$ for the continuous case, and $P = dI_b V_b$ for the pulsed beam. In reality, the electrical load on the spacecraft will exceed this value. Many components of a pulsed electron beam require constant power, so the efficiency for the pulsed beams is likely lower than this analysis shows.

In Fig. 3, the average force produced by a given set of parameters is plotted against the power required to operate that electron beam. The blue points represent continuous beam cases, and the red points represent pulsed cases. Each pair of points has a unique set of parameters (R_T, R_D, I_b, V_b, T_p, and d) that differ only in the duty cycle.

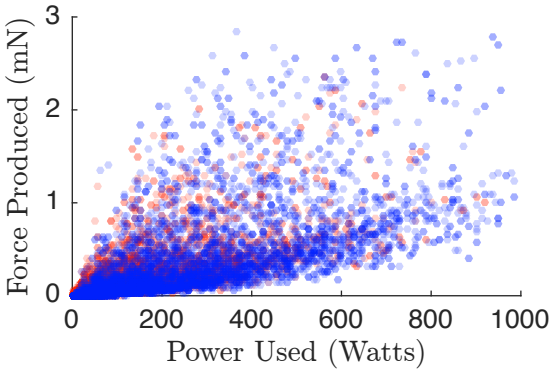

Figure 3. Comparison of force produced by continuous (blue) and pulsed (red) beams plotted agains the power in the beam

The efficiency can be found by taking the ratio of the force (y axis) to the power in the beam (x axis). This amounts to the slope of a line stretching from the data point to the origin. A higher slope means a higher efficiency. Although difficult to see at this scale, the pulsed cases consistently have higher efficiency below about 50 Watts. This lead in efficiency would likely be tempered by more realistic electron gun models.

It may be the case that our tug spacecraft is not power limited but voltage limited. At sufficiently high voltages, sharp corners on either spacecraft may arc into the ambient plasma through coronal discharge. A high energy beam may also cause Bremsstrahlung, where the deceleration of an electron releases high-energy photons in the X-ray range that could seriously damage spacecraft electronics. Fig. 4 shows the force produced by a beam of a given voltage. Blue once again represents the continuous cases while red represents the pulsed.

There is a very strong quadratic limit in the maximum force that can be produced for a given voltage. This matches the findings of Schaub & Sternovsky [18] that the maximum force between two equal-radius charged spherical spacecraft in vacuum that employ an electron

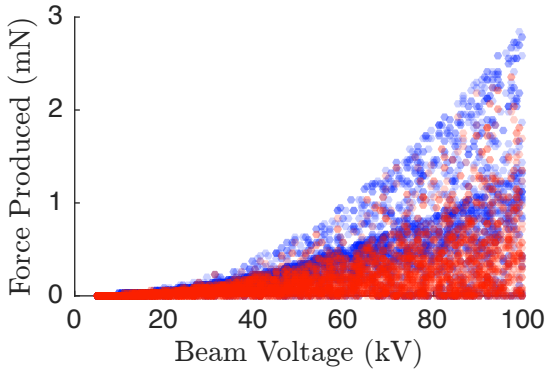

Figure 4. Comparison of force produced by continuous (blue) and pulsed (red) beams plotted agains the voltage of the beam

gun with accelerating voltage of V is

$$F_{\max} = \frac{4\pi\epsilon_0 R_{\mathrm{T}} R_{\mathrm{D}}}{(r - R_{\mathrm{T}})(r - R_{\mathrm{D}})} \frac{V^2}{4} \tag{19}$$

Where $k_c = 1/4\pi\epsilon_0$ and the spacecraft are separated by r. For our analysis we used the center-to-center separation $r = 5(R_{\mathrm{D}} + R_{\mathrm{T}})$, inserting this yields:

$$F_{\max} = \frac{4\pi\epsilon_0 R_{\mathrm{T}} R_{\mathrm{D}}}{80R_{\mathrm{T}}^2 + 164R_{\mathrm{T}}R_{\mathrm{D}} + 80R_{\mathrm{D}}^2} V^2 \tag{20}$$

The maximum of this force occurs when the craft are equally sized and is independent of the actual sizes. This is only because small craft are closer together. Using equally sized spacecraft yields:

$$F < \frac{4\pi\epsilon_0}{324} V^2 \tag{21}$$

$$F < 3.434 * 10^{-13}\ V^2 \tag{22}$$

Where F is in Newtons and V is in Volts. For a 100 kV beam, the theoretical maximum is 3.43 mN. We can also find a quadratic curve to bound our Monte Carlo data and compare with our analytic result. The maximum force within each of 50 equally sized bins ranging from 5 to 100 kV along with the bin centers is used as the bounding line. Constraining the curve to be quadratic gives us the following maximum:

$$F < 3.299 * 10^{-13}\, V^2 \tag{23}$$

This number is very close to the predicted maximum. Furthermore, the 95% confidence bounds ($3.146 * 10^{-13}, 3.452 * 10^{-13}$) include the analytic maximum.

5. RE-ORBITING ANALYSIS

An end objective of the ET includes re-orbiting debris to a graveyard orbit some 250 to 300 km above GEO. This process is mathematically modeled as a perturbation in the along-track direction which slowly changes the semi-major axis of the debris orbit. Schaub and Jasper [15] approximated the change in semi-major axis over 1 day as:

$$\Delta a = \frac{4\pi}{n^2} \frac{F}{m} \tag{24}$$

where n is the mean motion of the orbit [radians/second]. They went on to find this linear relationship between the effective radius (for capacitance matching) and launch mass.

$$m = (R - 1.152)/0.00066350 \tag{25}$$

where m_d is in kilograms, r_d is in meters, and the radius is between 1 and 6 meters. In this range it predicts masses between 1000 and 6000 kg. The launch mass is a conservative estimate of the actual mass as all of the station-keeping propellant is likely exhausted. The SMA rate is plotted against the power in the beam for both the pulsed and continuous beam cases in Fig, 5

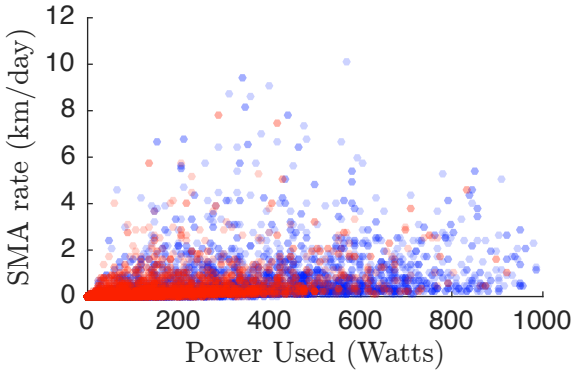

Figure 5. Comparison of SMA rate produced by continuous (blue) and pulsed (red) beams plotted agains the power in the beam

As a comparison to prior work, the fastest SMA rate is near 10 km/day, which translates to re-orbit times near 1 month rather than the 2-4 month estimates in earlier work. As with the force analysis, the pulsed cases are consistently more efficient below about 50 Watts or 5 km/day. To investigate a voltage-limited craft, the SMA rate is plotted against the beam voltage in Fig. 6.

The data once again has a quadratic bound, but this is not as striking a trend as the plot of force vs. voltage in Fig. 4. This bound can be analytically predicted by combining the SMA rate equation, Eq. (24), the mass-to-radius relationship, Eq. (25), and the force optimum found earlier, Eq. (20). When this is done the following SMA rate maximum is found:

$$\begin{aligned} \frac{\Delta a}{\text{day}} &< \frac{4\pi}{n^2} \frac{F}{m} \\ &< \frac{4\pi}{n^2} \frac{0.00066350}{(R_{\mathrm{D}} - 1.152)} \frac{4\pi\epsilon_0 R_{\mathrm{T}} R_{\mathrm{D}}}{80R_{\mathrm{T}}^2 + 164R_{\mathrm{T}}R_{\mathrm{D}} + 80R_{\mathrm{D}}^2} V^2 \end{aligned} \tag{26}$$

The SMA rate is maximized when the deputy mass is low and the force is high. This is done by making the deputy

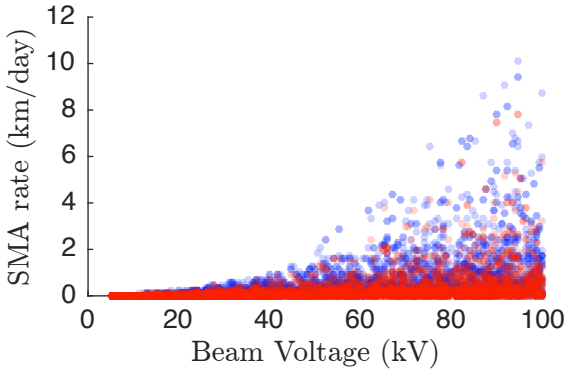

Figure 6. Comparison of SMA rate produced by continuous (blue) and pulsed (red) electron beams.

as small as possible and making the tug and deputy the same size, which gives both of them a radius of 1.5 m. This explains why the quadratic boundary was not seen as clearly – the force maximum is found when both radii are equal while the SMA rate maximum requires both radii be equal *and* small. The quadratic boundary would likely strengthen if we increased the number of Monte Carlo runs. If we insert this result, we arrive at the following theoretical bound in our range.

$$\frac{\Delta a}{\text{day}} < 1.5558 * 10^{-9}\ V^2 \tag{27}$$

Where Δa is in km and V is in Volts. For a beam of 100 kV, the maximum SMA rate is 15.58 km/day. Although the quadratic coefficient is not found from the Monte Carlo results, a parabola that begins at the origin and stretches to 15.58 km/day at 100 kV would bound all the data.

6. EQUAL POWER ANALYSIS

6.1. Single Power Level

If we constrain our analysis to a certain power and tug and debris sizes it changes the problem from six-dimensional to three-dimensional, two of which are non-physical for continuous beams. To investigate the highest force produced at different power levels, small departures from optimal continuous beam cases are considered. The power in a beam for a continuous and pulsed beam is given by,

$$P = I_{\text{b}_0} V_{\text{b}_0} = I_{\text{b}} V_{\text{b}}\ d \tag{28}$$

respectively, where a sub-subscript of 0 indicates the continuous case. If both beams are constrained to have the same power, the pulsed voltage and current must be raised since $d < 1$. A way to raise both the voltage and the current equally is:

$$I_{\text{b}} = \frac{I_{\text{b}_0}}{\sqrt{d}} \qquad V_{\text{b}} = \frac{V_{\text{b}_0}}{\sqrt{d}} \tag{29}$$

This deterministically allows for the effect of pulsing to be investigated in a one-dimensional manner. A degree of freedom is added to allow optimal tuning of the voltage and current:

$$I_{\text{b}} = \frac{\gamma I_{\text{b}_0}}{\sqrt{d}} \qquad V_{\text{b}} = \frac{V_{\text{b}_0}}{\gamma\sqrt{d}} \tag{30}$$

A γ value greater than 1.0 indicates that current increases more than voltage, and a value below 1.0 indicates that voltage increases more than current. The pulse period was not found to make a large difference in the range we looked at (0.1 – 1 s), so we randomized it and consider only the maximum force case. This allows us to look at the problem deterministically in two dimensions.

In the following analysis we considered the case of a 2 meter tug and a 1.5 meter deputy in nominal GEO space weather conditions separated by $\rho = 5(R_{\text{T}} + Rd) = 17$m and a power of 16 Watts. Baseline numbers for the continuous beam were taken from Hogan et. al. [10] as $V_{\text{b}} = 37$ kV and $I_{\text{b}} = 432\ \mu$A and produces a force of 0.2103 mN. To expand this, we will look at duty cycles of 10%, 25%, 50%, 75% and the continuous case, 100%. We will also look at γ values of 0.4, 0.4706, 0.5714, 0.7273, 1.0, 1.3750, 1.75, 2.125, and 2.5. These are spaced by having the first four numbers be the inverses of the last four, which gives us equal space to look at high voltage cases as high current cases. A plot of the max force subject to the the two deterministic parameters d and γ is shown in Fig. 7:

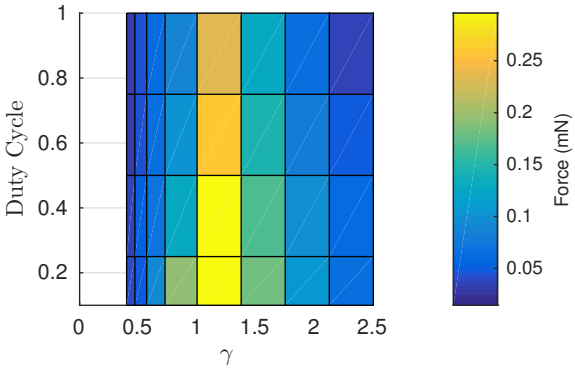

Figure 7. Force produced at 16 Watts subject to changing voltage, current, and duty cycle.

Each row of this plot has the same duty cycle – the top row represents a continuous beam and the bottom row represents a pulsed beam with a 10% duty cycle. The rows of the plot have the same γ value, meaning that the relative scaling of voltage and current is the same, although both increase by $1/d$ as one travels up a column. Using Eq. (30) allows us to see that current will be constant when $\gamma \propto \sqrt{d}$, which means that parabolas are level curves in current. Current is minimized in the bottom right corner, maximized in the upper left corner, and steps up along ever-steepening parabolas between them. Level curves in voltage are given by $\gamma \propto \sqrt{d}$ which in

our plot translates to $y \propto 1/x^2$. Voltage is minimized in the bottom left corner and maximized in the upper right.

The top row of Fig. 7 has a maximum near $\gamma = 1$ which indicates that our baseline parameters are close to optimal. The max force at lower duty cycles is also found with γ near 1, which gives a good starting point for optimizing the force.

6.2. Power Level Range

At 16 Watts, there is a clear benefit to pulsing – not only is the force increased by nearly 40%, but a 10% beam opens up 900 ms windows where both craft are uncharged and the beam is not operating. This would allow for control maneuvers and measurements to be made without interference from the electron beam. To investigate whether the force increase persisted at different power levels, this analysis was repeated at 2, 4, 8, 16, 32, 64 and 128 Watts. The baseline parameters (for the optimal continuous case) were hand-tuned and are given in Tab. 2.

Table 2. Baseline Continuous Beam Parameters

Power (W)	Voltage (kV)	Current (mA)
2	8	0.25
4	14	0.2857
8	25	0.32
16	37	0.4324
32	53	0.6038
64	75	0.8533
128	100	1.28

It is interesting to note that both the optimal beam voltage and current are approximately proportional to the square root of the power. The maximum force at each duty cycle was recorded and is shown in the log-log plot in Fig. 8.

Each color represents a different duty cycle, with green being a continuous beam and blue being a 10% duty cycle. There is a significant increase in force when using a pulsed beam at low power levels that decreases as the power rises. At 2 Watts, a 10% beam exceeds it's continuous counterpart by a factor of 2.14, but at 128 Watts, it is only 7.4% better. Additionally, these solutions offer 900 ms windows where both craft are discharged and the beam is not operating during which control maneuvers can be executed and measurements can be taken. Unfortunately, the high force and low duty cycle cases require very high beam voltages – the optimal solution for all cases at or above 16 Watts uses more than 100 kV. The optimal γ value was also found at each power level and duty cycle. At low powers and low duty cycles γ is larger than 1 in the max force case, which translates to more current increase than voltage increase. It was equal to 1.0 for all powers larger than or equal to 8 Watts.

The voltage in a pulsed beam grows with $\gamma/\sqrt{d}$. The average force is proportional to both V^2 and d. Combining

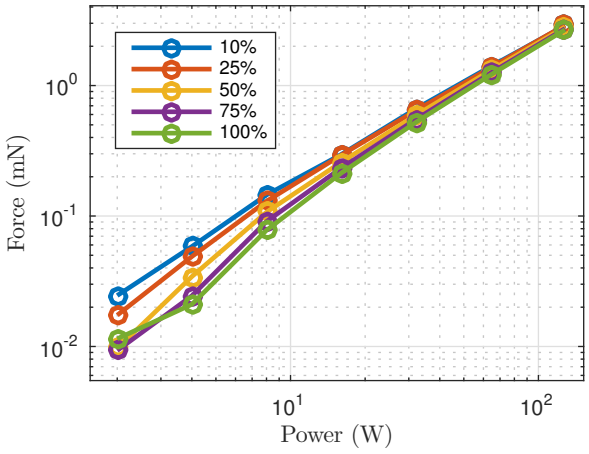

Figure 8. Maximum force at a variety of power levels as a function of power.

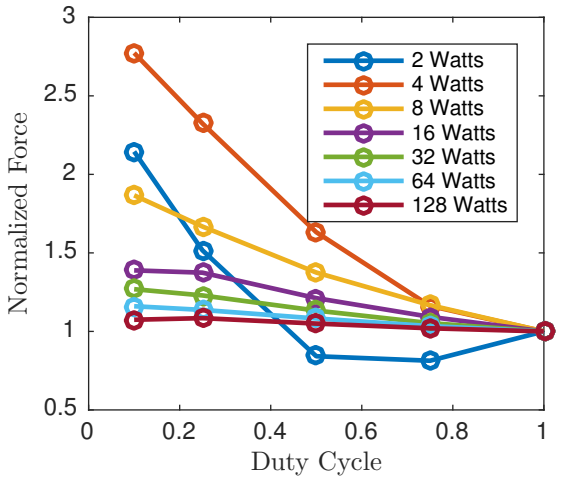

Figure 9. Maximum force at a variety of power levels as a function of duty cycle.

these results makes the average force proportional only to γ^2, since the duty cycle factors out. However, γ is larger than 1 for low powers and low duty cycles, which predicts a strong force increase in this regions. The highest force for each duty cycle at different power levels is divided by the continuous force at that same power level and plotted in Fig. 9.

The low power (red, blue, and yellow) curves do indeed have a strong increase at low duty cycle, while the higher power curves do not. In this analysis, γ jumps from 1.0 to 1.375, a higher-resolution spread could change these findings slightly. Future work will investigate these effects.

7. CONCLUSION

The traditional current balance equation is changed to include a pulsed beam that is allowed to escape the system completely for a certain energy band. Six parameters ($R_{\rm T}, R_{\rm D}, V_{\rm b}, I_{\rm b}, T_{\rm p}, d$) are selected to vary in a Monte Carlo analysis. An analytic upper bound for the force between two spacecraft as a function of beam voltage is found, and has good agreement with the Monte Carlo results. At low power levels, a pulsed ET is found to be more efficient than a continuous one. The results are then applied to orbit raising for both power and voltage-limited spacecraft. The pulsed ET was also more efficient for semi-major axis raising at low power levels. A similar analytic upper bound for the semi major axis rate as a function of beam voltage was found. This limit also has good agreement with the Monte Carlo results. The main limiting factor for both SMA rate and force is the voltage of the beam.

A deterministic equal power analysis is done for continuous and pulsed beams at 2, 4, 8, 16, 32, 64, and 128 Watts. Force increases at all of these power levels are achieved using low duty cycles, but require very high voltage beams at high power. The baseline current and voltage are found to vary with the square root of the power, and the optimal γ was found to increase with duty cycle at low power levels.

Pulsing the electron beam in the Electrostatic Tractor offers force increases for the same power, and creates windows of opportunity during which control maneuvers can be executed and measurements can be taken without interference from the electron beam. This allows for faster re-orbiting of GEO debris objects that are currently increasing the risk of collision in a very valuable orbital region.

REFERENCES

[1] Anderson, P. V. & Schaub, H. 2013, in 6th European Conference on Space Debris, ESOC, Darmstadt, Germany, paper No. 3a.P-3

[2] Anderson, P. V. & Schaub, H. 2013, Advances in Space Research, 51, 2195

[3] Bennett, T. & Schaub, H. 2014, in AAS/AIAA Spaceflight Mechanics Meeting

[4] Bennett, T., Stevenson, D., Hogan, E., McManus, L., & Schaub, H. 2014, in 3rd European Workshop on Space Debris Modeling and Remediation, CNES, Paris

[5] Chrystal, P., McKnight, D., Meredith, P. L., et al. 2011, Space Debris: On Collision Course for Insurers?, Tech. rep., Swiss Reinsurance Company Ltd, Zürich, Switzerland

[6] Fennell, J. F., Koons, H. C., Leung, M., & Mizera, P. 1983, 1983., 3

[7] Früh, C., Ferguson, D., Lin, C., & Jah, M. 2013, International Astronautical Congress, 64

[8] Galabova, K. K. 2004, PhD thesis, Massachusetts Institute of Technology, Cambridge, MA

[9] Griffiths, D. J. 1999, Introduction to Electrodynamics, 3rd edn. (Prentice Hall)

[10] Hogan, E. A. 2014, Advances in Space Research, 55, 630

[11] Lai, S. T. 2011, Fundamentals of Spacecraft Charging: Spacecraft Interactions with Space Plasmas (Princeton University Press)

[12] Moorer, D. F. & Schaub, H. 2011, Electrostatic Spacecraft Reorbiter, US Patent 8,205,838 B2

[13] Peck, M. A. 2005, in AIAA Guidance, Navigation and Control Conference, San Francisco, CA, paper No. AIAA 2005-5995

[14] Peck, M. A., Streetman, B., Saaj, C. M., & Lappas, V. 2007, Journal of British Interplanetary Society, 60, 263

[15] Schaub, H. & Jasper, L. E. Z. 2013, AIAA Journal of Guidance, Control, and Dynamics, 36, 74

[16] Schaub, H. & Moorer, D. F. 2014, The Journal of the Astronautical Sciences, 59, 161

[17] Schaub, H. & Sternovsky, Z. 2013, in 6th European Conference on Space Debris, ESOC, Darmstadt, Germany, paper No. 6b.O-5

[18] Schaub, H. & Sternovsky, Z. 2013, Advances in Space Research, 53, 110

[19] Stevenson, D. & Schaub, H. 2013, Advances in Space Research, 51, 10

[20] Stevenson, D. & Schaub, H. 2013, in 5th International Conference on Spacecraft Formation Flying Missions and Technologies, Münich, Germany

[21] Stiles, L. A., Seubert, C. R., & Schaub, H. 2012, in AAS Spaceflight Mechanics Meeting, Charleston, South Carolina, Paper AAS 12

[22] Streetmann, B. & Peck, M. A. 2009, Journal of Guidence, Control, and Dynamics, 32